Journal of Photochemistry and Photobiology A: Chemistry 199 (2008) 1–7

Contents lists available at ScienceDirect

Journal of Photochemistry and Photobiology A: Chemistry

journal homepage: www.elsevier.com/locate/jphotochem

Syntheses of NiO nanoporous films using nonionic triblock co-polymer templates and their application to photo-cathodes of p-type dye-sensitized solar cells

Seiichi Sumikura, Shogo Mori, Shinya Shimizu, Hisanao Usami, Eiji Suzuki*

Department of Fine Materials Engineering, Faculty of Textile Science and Technology, Shinshu University, 3-15-1 Tokida, Ueda, Nagano 386-8567, Japan

ARTICLE INFO

Article history:
Received 11 November 2007
Received in revised form 8 March 2008
Accepted 8 April 2008
Available online 16 April 2008

Keywords:
Template
Co-polymer
Nanoporous NiO
Dye-sensitization
p-type

ABSTRACT

We prepared nanoporous NiO films from $NiCl_2$ in water/ethanol mixed solution, using a series of polyethyleneoxide–polypropyleneoxide–polyethyleneoxide (PEO–PPO–PEO) triblock co-polymers as template, and examined them as p-type NiO electrodes sensitized with a merocyanine dye. Triblock co-polymers with high PEO/PPO ratio leaded to three-fold higher photocurrent in comparison with low PEO/PPO polymers. Use of high PEO/PPO templates resulted in NiO membrane structure formed by uniformly distributed NiO nano particles with small interparticle voids, giving large surface area for dye adsorption, while low PEO/PPO templates resulted in larger void volume and less surface area. Photocurrent under simulated solar light was sum of the currents generated by NiO direct excitation and by dye-sensitization at spectra below 450 nm and from 450 to 590 nm, respectively.

1. Introduction

Since a dye-sensitized solar cell (DSC) with 7% solar to power conversion efficiency was reported by O'Regan and Grätzel in 1991 [1], DSCs have attracted attention due to their reasonable efficiency and expected low production cost. Typically a DSC is composed of a dyed porous film of nanocrystalline titanium dioxide, an n-type semiconductor, interpenetrated by a liquid electrolyte containing an I^-/I_3^- redox couple, and a counter electrode such as platinum-coated fluorine-doped tin oxide (FTO). Because of n-type behavior of titanium oxide electrode, the conventional DSC is called n-DSC in this work. To date, the highest conversion efficiency above 11% has been achieved with n-DSC using Ru complex dye, which converts photons in solar spectrum between 400 and 650 nm to current at high efficiency ranging from 68 to 87% [2].

In order to increase the solar to power efficiency further, wider solar light spectrum should be harvested. However, it is not trivial to design single dye absorbing wide range of the spectrum. In addition, to exploit lower energy photons of near IR region, open-circuit voltage (V_{OC}) of the solar cells must be decreased. A remedy of the issues is to introduce tandem structure to DSCs [3–5].

In 2000, He et al. reported a tandem solar cell using dye-sensitized TiO_2 as a photo-anode and dye-sensitized NiO, a p-type semiconductor, as a photo-cathode for longer wavelength spectrum [5]. Dye-sensitization of the photo-cathode occurs due to hole injection from the photo-excited dye to the NiO. The photo-anode and -cathode were connected in series through an electrolyte containing I^-/I_3^- redox couple. For the case, V_{OC} is the potential difference between the Fermi levels of the TiO_2 and NiO, and higher than that of conventional DSCs. In solar spectrum, number of photons available for the photo-cathode is almost equal to that for the conventional photo-anode, which assures tandem cells of current density almost equal to the conventional n-DSCs. Hence due to a higher V_{OC} at the similar level of current density, a better efficiency can be expected for the tandem DSCs than conventional ones.

At the moment, however, efficiency of dye-sensitized p-type metal oxide semiconductor cell is very low, which limits the efficiency of the tandem cell using dye-sensitized n- and p-type metal oxide electrodes (n/p-DSCs). The highest reported values for dye-sensitized p-type metal oxide solar cells (p-DSC) using NiO were 1 mA cm^{-2} of J_{SC} and 80 mV of V_{OC} [6,7]. Therefore, development of more efficient dye-sensitized p-type semiconductor electrode is important.

In case of conventional DSC, particle and pore sizes of nanoporous TiO_2 membrane have significant influence on cell performance [8]. Smaller particle size is preferable to large specific surface area for adsorbing dye, while larger particle size is so to lowering electron transfer barrier at particle interfaces. For penetration of dye and electrolyte into TiO_2 nanoporous membrane, larger pore size is favorable, while smaller pore volume is so for obtaining larger specific surface area of the membrane. For conventional n-DSC, particle and pore sizes have been optimized to some

* Corresponding author. Tel.: +81 268 21 5456; fax: +81 268 21 5456.
E-mail address: esuzuki@shinshu-u.ac.jp (E. Suzuki).

1010-6030/$ – see front matter © 2008 Elsevier B.V. All rights reserved.
doi:10.1016/j.jphotochem.2008.04.007

Table 1
Constitution of applied triblock co-polymer $PEO_mPPO_nPEO_m$

Polymer	m	n	MW	m/n	Group
F88	104	39	11400	2.67	F
F108	133	50	14600	2.66	
P105	37	56	6500	0.66	P
P123	20	69	5750	0.29	

extent [8], while almost no optimization has been tried yet in case of nanoporous NiO membrane for p-DSC. In this work, therefore, we examined effects of particle and pore sizes of NiO membrane on the p-DSC performance.

There has been reported that nonionic triblock co-polymers were successfully applied as templates for nano-pores of silica [9], titania [10] and tin oxide [11]. In this work, we applied a series of polyethyleneoxide–polypropyleneoxide–polyethyleneoxide (PEO–PPO–PEO) triblock co-polymers as template for preparing nanoporous NiO membrane, expecting that particle and pore sizes of the membrane can be adjusted by applying the co-polymers with various PEO/PPO ratio and molecular size, or by changing $NiCl_2$/polymer ratio.

2. Experimental

2.1. Materials

Anhydrous nickel chloride, dried ethanol, dried acetonitrile (Wako Pure Chemicals, Ltd.), lithium iodide, iodine (Aldrich) and merocyanine dye (3-carboxylmethyl–5–[2-(3-octadecyl-2(3H)-benzothiazolylidene)ethylidene]-2-thioxo-4-thiazolidinone, NK-2684, Hayashibara Biochemical Laboratories, Ltd.) were used as received. Polyethyleneoxide–polypropyleneoxide–polyethyleneoxide triblock co-polymers, F88, P105, F108 and P123, were kindly supplied from BASF Japan, Ltd. and used as received. Molecular constitution of the polymers is shown in Table 1, where the polymers having longer PEO chains are classified in F group, and those having shorter PEO chains are in P group. Milli-Q water was used for solvent of $NiCl_2$ solution. Fluorine-doped tin oxide transparent electrodes (FTO, ca. 9.5 Ω/square) were kindly supplied by Nippon Sheet Glass Co., Ltd.

2.2. Preparation of porous NiO film

Standard precursor solutions of NiO were prepared by dissolving anhydrous $NiCl_2$ (1 g) and the triblock co-polymer (1 g) into a mixture of Milli-Q water (3 g) and ethanol (6 g); each solution was named after the corresponding polymer. For F88, a solution with a larger ratio of $NiCl_2$ to polymer (1 g $NiCl_2$, 0.3 g polymer) and another solution with a smaller ratio of $NiCl_2$ to polymer (0.3 g $NiCl_2$, 1 g polymer) were prepared and named F88L and F88S, respectively (Table 2). The solution was left at rest for 3 days at 30 °C, and then centrifuged. Obtained supernatant solution was deposited on an FTO glass substrate by doctor blade method using mending tape (Scotch®) as a spacer, and dried at room temperature. The dried film was then calcined in air at 400 °C for 0.5 h.

Table 2
Amount of polymer and $NiCl_2$ in the 3 g water and 6 g ethanol mixed solvent

	Polymer [g]	$NiCl_2$ [g]	$NiCl_2$/polymer
F88	1	1	1.0
F108	1	1	1.0
P105	1	1	1.0
P123	1	1	1.0
F88L	0.3	1	3.3
F88S	1	0.3	0.3

2.3. Characterization of NiO films

The film was characterized by X-ray diffraction (Rigaku RINT system, Cu Kα) and the crystal size was estimated by applying the Scherrer formula on the diffraction peak. Morphology of the NiO film was examined by field emission scanning electron microscopy (FE-SEM; HITACHI S-5000). Film thickness was measured with surface profiler (Dektak 6M, ULVAC EQUIPMENT SALES, Inc.).

Specific surface areas were measured by BET method using a N_2 sorption isotherm (BELSORP 18, BEL Japan Inc.).

Film porosity P_F was calculated by Eq. (1).

$$P_F = 1 - \frac{M_F}{V_F \times \rho}, \quad (1)$$

where M_F is film mass, V_F film volume, and ρ NiO crystal density, 6.96 g cm^{-3}.

Surface area per volume, S_V, was calculated by Eq. (2).

$$S_V = \frac{(1 - P_F)S_{BET}}{V_{NiO}}, \quad (2)$$

where S_{BET} is specific surface area determined by BET method, and V_{NiO} is volume of NiO per mass, 0.1437 cm^3 g^{-1}.

2.4. Characterization of dye

The highest occupied molecular orbital (HOMO) and the lowest unoccupied molecular orbital (LUMO) potentials of the NK-2684 dyes were determined as follows. Oxidation potentials of ground state dyes were measured by cyclic voltammetry (CV) using an electrochemical analyzer (model 650A, ALS instruments), and used as the HOMO potential in our study. Reference electrode was Ag/AgCl, and working and counter electrodes were Pt wires. The optical absorption spectra in the range 300–900 nm was recorded with spectrophotometer (U-4100; HITACHI, Ltd.). Fluorescence spectrum measurement (F-4500; HITACHI, Ltd.) was carried out for the solutions containing 0.1–0.01 mM of the dyes in a quartz cell. They were bubbled with nitrogen gas for 5 min before measurements. Stray light was cut with a bandpass filter. The energy gap of dye (E_g) was calculated from Eq. (3) with short wavelength

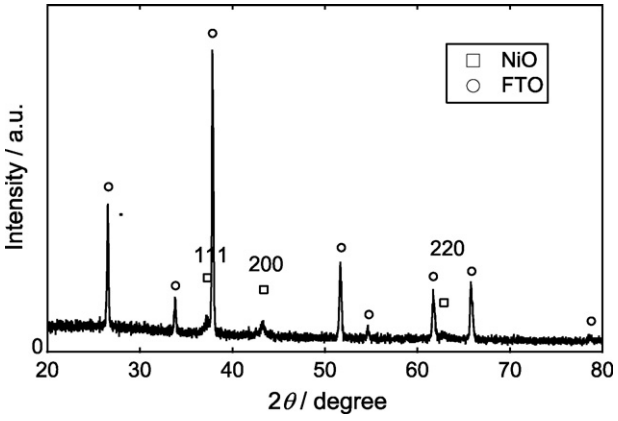

Fig. 1. Wide angle XRD pattern of NiO synthesized using F88 triblock co-polymer as template.

of fluorescence edge (λ).

$$E_g = \frac{1240}{\lambda}(\text{eV}), \quad (3)$$

where λ (nm) is the wavelength of the fluorescence edge. LUMO potential was calculated by using Eq. (4).

$$V_{LUMO} = V_{HOMO} - E_g \quad (4)$$

2.5. Fabrication and characterization of p-DSCs using NiO films

The NiO film was soaked in an ethanol solution of NK-2684 dye (0.05 mM) for 3 h at 60 °C and washed with acetonitrile to remove the excess dye. Cells were fabricated by coupling face to face a dyed or non-dyed NiO electrode and Pt sputtered FTO glass as a counter electrode, and by filling between two electrodes an electrolyte containing 0.05 M I_2 and 0.7 M LiI in acetonitrile (I^- rich electrolyte). Electrolyte containing 0.65 M I_2 and 0.7 M LiI in acetonitrile (I_3^- rich electrolyte) was also used to enhance electron transfer rate from NiO to I_3^-. *I–V* characteristics were measured using solar simulator (AM1.5 100 mW cm^{-2}, YSS-100, Yamashita Denso Co. Ltd.) and a cyclic voltammetry tool (HSV-100; Hokuto Denko Co., Ltd.). For incident photon to current conversion efficiency (IPCE) measurement, DSCs were irradiated with monochromatic light (SM-25, Bunkoh-Keiki Co. Ltd.) and generated short-circuit current was measured with a digital multimeter (model 2400, Keithley Instruments Inc.). IPCE was obtained by Eq. (5).

$$\text{IPCE}(\%) = 1240\frac{J_{SC}}{\lambda\phi} \times 100, \quad (5)$$

where J_{SC} is short-circuit current density (mA cm^{-2}), λ wavelength of monochromatic light (nm), and ϕ intensity of monochromatic light (mW cm^{-2}). Solar to power conversion efficiency η was calculated by Eq. (6)

$$\eta(\%) = \frac{J_{SC} \times V_{OC} \times \text{ff}}{I_0} \times 100, \quad (6)$$

where I_0 is the photon flux, 100 mW cm^{-2} for AM 1.5 in this work, J_{SC} is the short-circuit photocurrent density under irradiation,

Table 3
Particle size calculated by the Scherrer formula using XRD data and BET surface area

Polymer	Primary particle size [nm]	$NiCl_2$/polymer	BET surface area [m^2 g^{-1}]
F88	18.6	1.0	41.7
F88L	23.0	3.3	32.4
F88S	15.3	0.3	61.0
F108	12.0		43.6
P105	19.0		39.0
P123	20.4		22.8

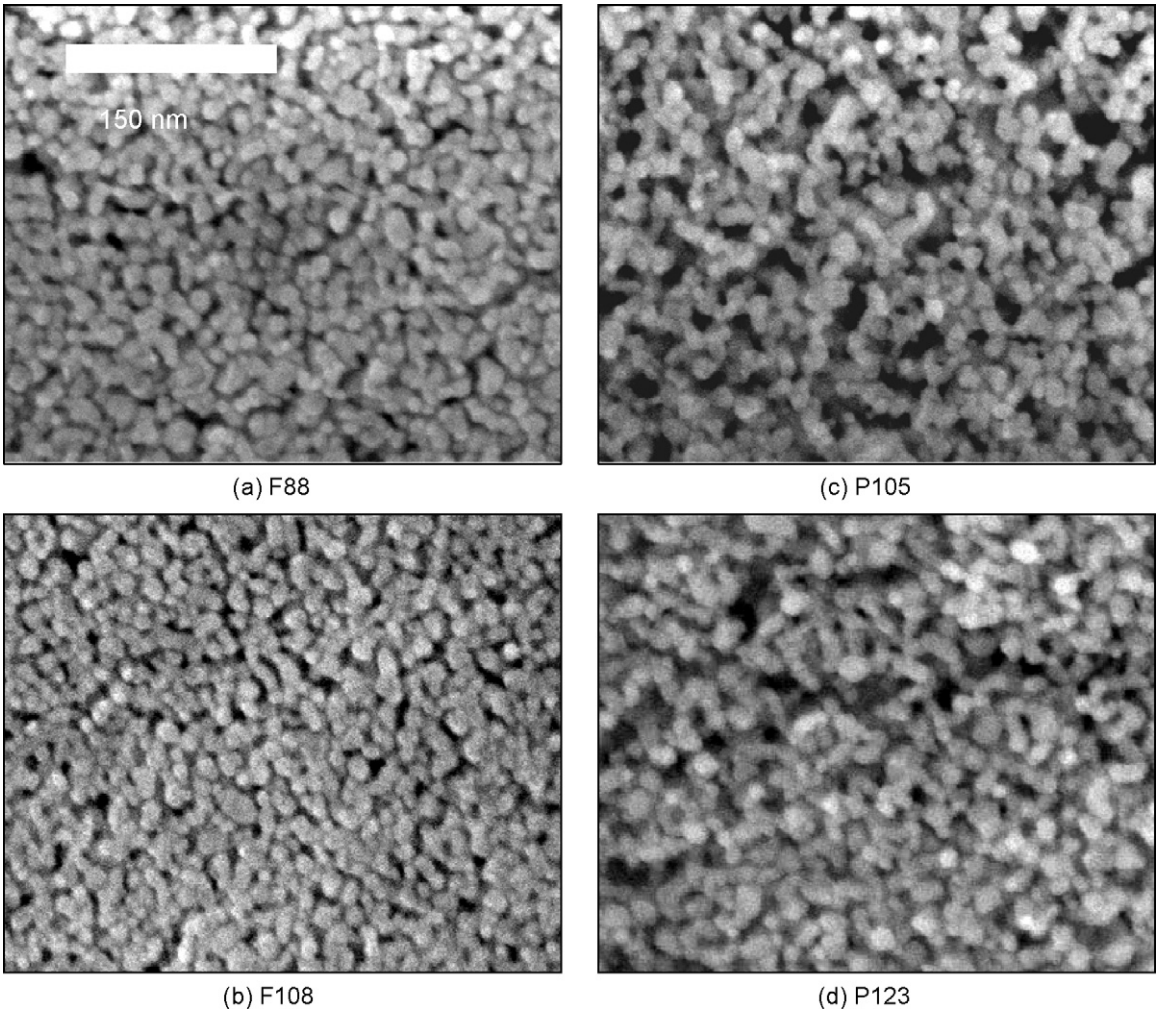

Fig. 2. FE-SEM images of nanoporous NiO films synthesized using F group polymers (a and b) and P group polymers (c and d).

V_{OC} is the open-circuit photovoltage (V), and ff represents the fill factor.

3. Results and discussion

3.1. Characterization of NiO films

The film thickness was adjusted to around 0.5 μm by tuning the spacer thickness. XRD pattern of NiO film prepared using F88 polymer template is shown in Fig. 1. There are three major diffractions assigned to the (1 1 1), (2 0 0) and (2 2 0) diffractions of a face centered cubic NiO crystals. The other NiO films showed the similar XRD patterns. The polymer constitution did not affect the lattice constant. The crystalline size estimated from the half width of the (2 0 0) major diffractions by applying the Scherrer formula ranged from 12.0 to 23.0 nm, and is shown in Table 3.

Fig. 2 shows FE-SEM images of NiO film. All the images exhibited nanoporous structure formed by nano particles and voids surrounded by them. Particle and void sizes are rather uniform, which suggested presence of long ordered meso-structure composed of Ni species and polymer before calcination. Most of the particles in the SEM image of F88-NiO are 10–20 nm in size, which is consistent with the size calculated using the diffraction peak width. This agreement indicated the particles are not crystalline aggregates, but individual crystals. P group polymers, P105 and P123, seemed to make larger voids than F group, which is tentatively explained as follows. The mixed solvent of water and ethanol is hydrophilic, and P group polymers, in which hydrophobic PPO segment is much larger than hydrophilic PEO segments, make large coagulated hydrophobic cores in the hydrophilic solvent. The polymer cores become large voids after calcination. In contrast, F group polymers, F88 and F108, which have large hydrophilic PEO segments, tend to disperse uniformly, forming small PPO cores. Hence small voids are left after calcination. Ni species residing in the hydrophilic environment constituted by the solvent and PEO segments become particles after solvent vaporization and then NiO crystalline particles upon calcination.

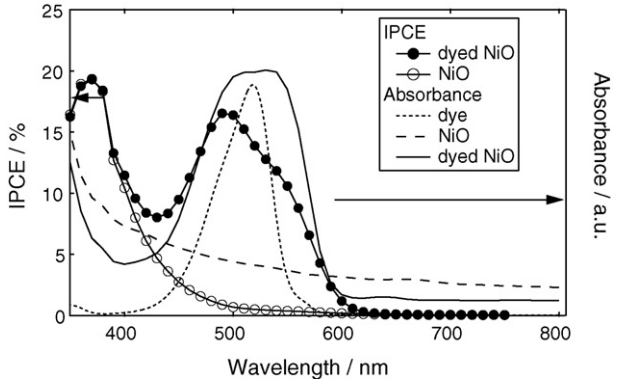

Fig. 3. Photocurrent action spectra of solar cells with the I^- rich electrolyte and the dyed or non-dyed NiO electrodes prepared using F88 polymer template, and absorbance of NK-2684 dye in ethanol, the non-dyed NiO film, and the dyed NiO film.

The crystalline size increased with increasing ratio of $NiCl_2$/polymer in series of F88S-, F88- and F88L-NiO films as shown in Table 3. F108, which has longer PEO chains, also yielded small crystals (12 nm on average). As a whole, lower ratio of $NiCl_2$/PEO seemingly tends to yield smaller crystals.

S_{BET}, specific surface area of NiO film determined by BET method, is shown in Table 3. S_{BET} is larger for F group than P group, which is consistent with the fact that F group NiO has smaller particle size and void volume than P group NiO.

3.2. Photo-electrochemical characterization of dyed and non-dyed NiO cells

IPCE and I–V performance of the cells with the dyed and non-dyed NiO electrodes prepared by using F88 polymer as a template were shown in Figs. 3 and 4, respectively. Observed photocurrent direction was cathodic with respect to the NiO electrodes, and hence the cells are termed p-type cells in this work.

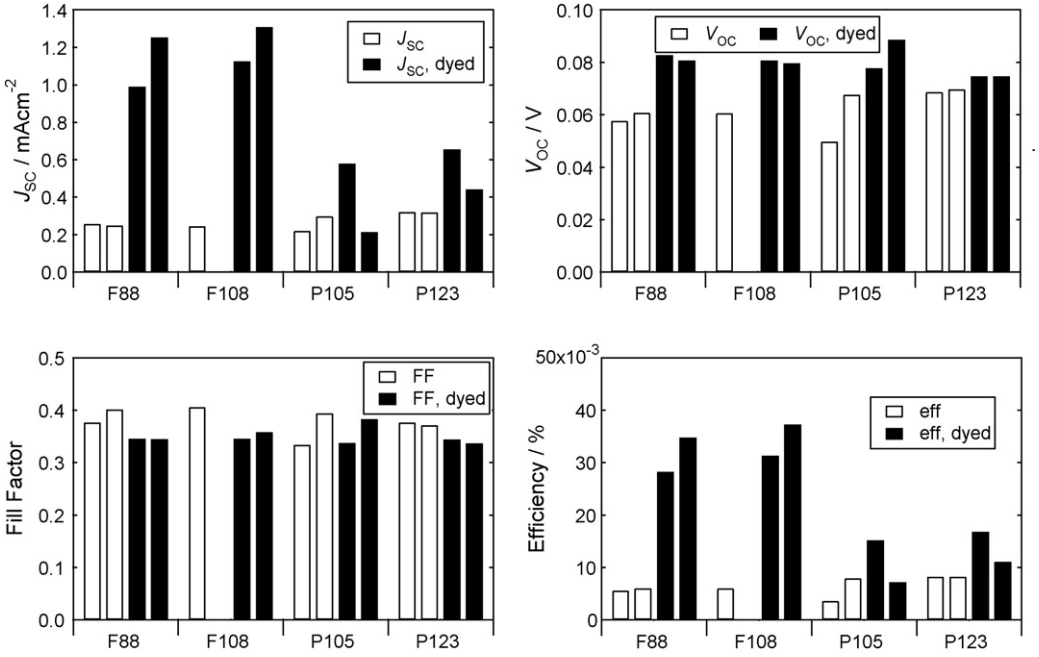

Fig. 4. I–V performances of the solar cells with I^- rich electrolyte and the dyed and non-dyed NiO electrodes prepared using different polymer templates. One of the two non-dyed F108 cells did not function as a photovoltaic cell due to some failure during cell preparation.

3.2.1. Direct excitation vs. dye-sensitization

The non-dyed NiO cell exhibited a broad IPCE peak ranging from 300 to 450 nm and peaking at 370 nm. The high absorbance of the NiO at below 450 nm shown in Fig. 3 and the low light transmittance of the FTO glass at below 300 nm seemingly worked cooperatively for forming this IPCE peak. Hence we attributed the IPCE peak to direct excitation of NiO semiconductor.

The dye NK-2684 used in this work had exhibited comparatively high solar to power conversion efficiency among the six kinds of dyes applied to NiO electrodes in the authors' laboratory (in preparation). NK-2684 dye absorbs photons with wavelength between 450 and 600 nm and photo-generated holes in HOMO of the dye are injected into NiO valence band, generating photocurrent. The dyed NiO cell exhibited two IPCE peaks, one at 370 nm and the other at 500 nm. The former is due to the direct excitation of NiO. The latter can be attributed to dye-sensitization, since the peak wavelength of the latter is close to the absorption maximum wavelength of the dye shown in Fig. 3.

The dyed NiO exhibited V_{OC} higher than non-dyed one by some unknown mechanism. A possible explanation on this V_{OC} increase is the following. The dye adsorption on NiO decreased the NiO/electrolyte interface area, resulting in suppression of backward transfer of the holes from NiO to the electrolyte. As a result, Fermi level of NiO positively sifted, increasing V_{OC}, the difference between Fermi level of NiO and I^-/I_3^- redox potential.

The direct excitation IPCE peak is as large as the dye-sensitized one. In solar light, however, there are far less photons with wavelength short enough to excite NiO, in comparison with those for the dye-sensitization. Hence the performance of the dyed NiO cell is mainly owing to dye-sensitization and partly to direct excitation. Dye-sensitization increased the solar to power conversion efficiency six-fold as shown in Fig. 4 in comparison with the non-dyed cell.

The NiO valence band edge potential V_{VB} is 0.54 V vs. NHE [6] and the band gap energy E_g is 3.2 eV, which was estimated by Eq. (7) using the reported absorption data [12].

$$(\alpha h\nu)^n = A(h\nu - E_g), \tag{7}$$

where A is an arbitrary constant, n is 1/2 for the indirect band transition.

The absorption edge corresponding to E_g of 3.2 eV is estimated at 390 nm. The conduction band edge potential V_{CB} was estimated at −2.7 V vs. NHE by $V_{CB} = V_{VB} - E_g$. The redox potential of I^-/I_3^- is 0.44 V vs. NHE [13]. These potential data are shown in Fig. 5.

The direct excitation photocurrent at around 370 nm can be explained using these potential data as follows. Photo-excited electrons and holes are generated in NiO when irradiated with light of 390 nm and shorter wavelength. Due to p-type property of NiO semiconductor, the electrons tend to move to the NiO surface, and there react with I_3^- yielding cathodic current, while the holes can travel through NiO to the FTO electrode.

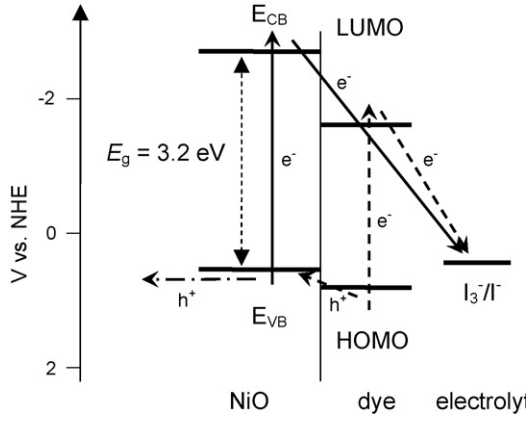

Fig. 5. Energy diagram of p-DSC using NiO electrode dyed with NK-2684.

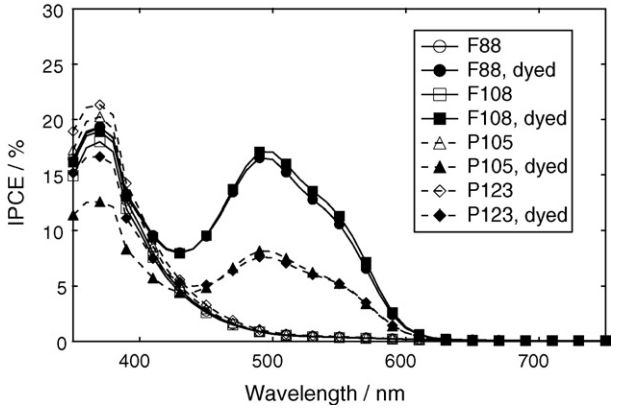

Fig. 6. Photocurrent action spectra of solar cells with I^- rich electrolyte and the dyed or non-dyed NiO electrodes prepared using different polymer templates.

Table 4
Adsorbed dye amount and surface area per volume (S_V) of NiO electrodes prepared using F88 or P105 and IPCE of DSCs

Polymer	Dye adsorption [μmol cm^{-3}]	IPCE at 500 nm [%]	S_V [m^2 cm^{-3}][a]
F88	450	16.4	68.8
P105	240	8.1	40.7

[a] S_V was calculated using BET surface area and porosity.

HOMO and LUMO potentials of the dye, V_{HOMO} and V_{LUMO}, are 0.81 and −1.60 V vs. NHE. Energy gap between HOMO and LUMO is 2.41 eV and consistent with the absorption maximum wavelength 515 nm of the dye in this work. V_{HOMO} is sufficiently deeper than the valence band edge to inject photo-generated holes from the dye to the valence band of NiO [14]. V_{LUMO} is deeper than the conduction band edge of NiO, and hence photo-excited electrons in the LUMO cannot be injected to the conduction band, while they can react with I_3^- in the electrolyte. Thus the observed cathodic dye-sensitization of NiO with NK-2684 dye is consistent with the potential data shown in Fig. 5.

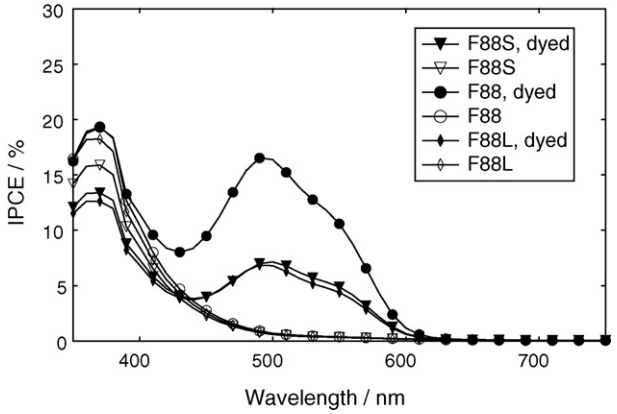

Fig. 7. Photocurrent action spectra of solar cells with I^- rich electrolyte and the dyed or non-dyed NiO electrodes prepared using F88 polymer template at different $NiCl_2$/polymer ratios.

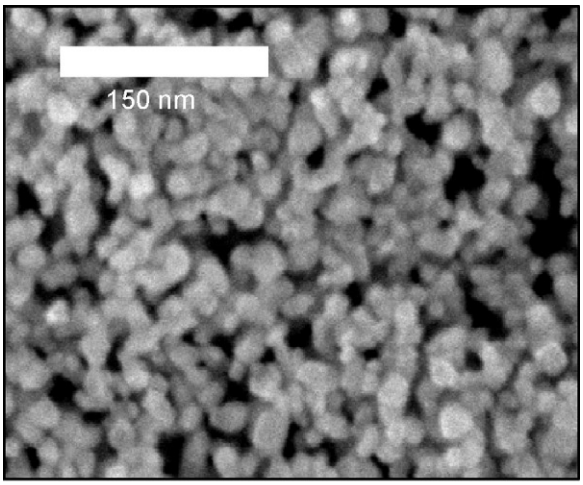

(a) F88S

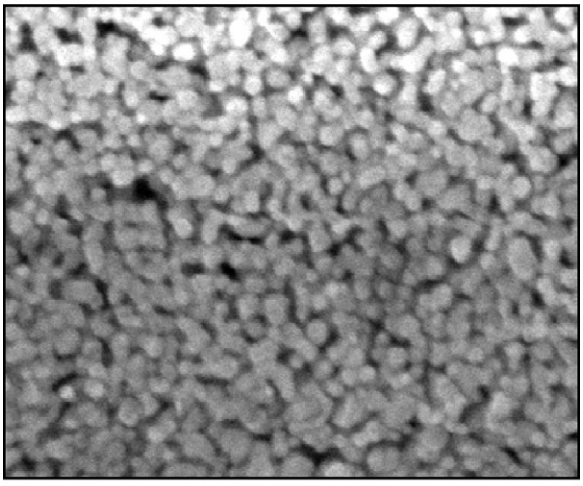

(b) F88

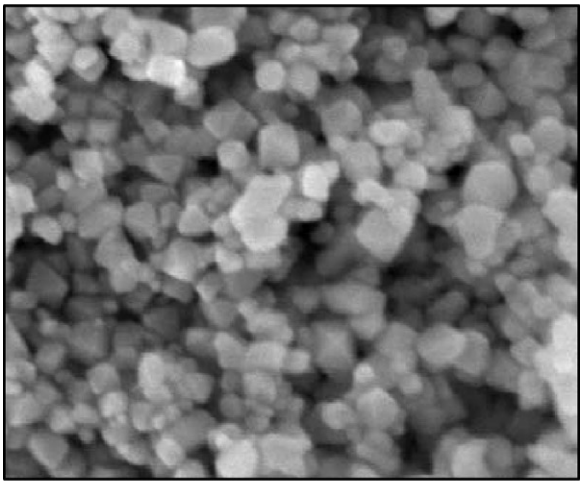

(c) F88L

Fig. 8. FE-SEM images of nanoporous NiO films synthesized using F88 polymer template at different NiCl2/polymer ratios. (a) F88S, (b) F88, and (c) F88L.

3.2.2. Effect of template type on cell performance

Fig. 6 shows the dependency of IPCE on type of the template polymer. F group polymers led the DSCs to a dye-sensitization IPCE peak 1.9 times as high as P group. Amount of adsorbed dye was measured as described in Section 2 and reported in Table 4. The dye amount adsorbed on F88-NiO (F group) electrode was twice as much as on P105-NiO (P group), which explains the two-fold IPCE of F group. P group NiO involves much larger pore than F group NiO as shown in Fig. 2. Hence P group NiO was thought to have less dye adsorption surface area. In fact, porosity of p105-NiO was estimated at 0.85, while that of F88-NiO was at 0.76, and the surface area per volume, S_V, of F88-NiO was estimated at 1.7-fold that of p105-NiO by Eq. (4) using BET surface area data in Table 3.

As a whole, F group demonstrated the solar to power conversion efficiency 2.5 times as high as P group (Fig. 4).

3.2.3. Effect of $NiCl_2$/polymer ratio on cell performance

Fig. 7 shows IPCE of cells with F88S, F88, and F88L-NiO films, of which $NiCl_2$/F88 mass ratio is 0.3, 1.0, and 3.3, respectively. F88-cells exhibited more than twice higher dye-sensitization IPCE than the others. The SEM images shown in Fig. 8 indicated that morphology of F88-NiO film featuring uniformly distributed nano particles and pores with small porosity is more favorable to DSC than that of the others.

F88L-NiO film looked opaque, and F88S-NiO film had many cracks, while F88-NiO film was transparent and had no cracks. These results suggested that optimum ratio of $NiCl_2$/F88 polymer is close to 1.0.

3.2.4. DSC performance with I_3^- rich electrolyte

The I_3^- rich electrolyte (0.65 M I_2 and 0.7 M LiI) was applied to improve electron transfer rate from NiO and the dye to I_3^- in the following experiment instead of I^- rich one (0.05 M I_2 and 0.7 M LiI) in the experiments reported above. IPCE and *I–V* performance were shown in Fig. 9 and 10, respectively, for the cells with the dyed and non-dyed NiO electrodes. Note that the IPCE range of Fig. 10 is 50%, while that of Fig. 4 is 25%.

Direct excitation IPCE at 370 nm increased from 19% to over 50% by applying I_3^- rich electrolyte in the case of non-dyed NiO; probably the higher I_3^- concentration enhanced the rate of electron transfer from NiO conduction band to I_3^-. Dye adsorption disturbed the increase of direct excitation IPCE; probably the dye partly covered NiO surface, reducing the NiO surface area available for electron transfer to the electrolyte.

Direct excitation IPCE of the non-dyed F group NiO at 500 nm was remarkably enhanced from 1 to 12% by using the I_3^- rich elec-

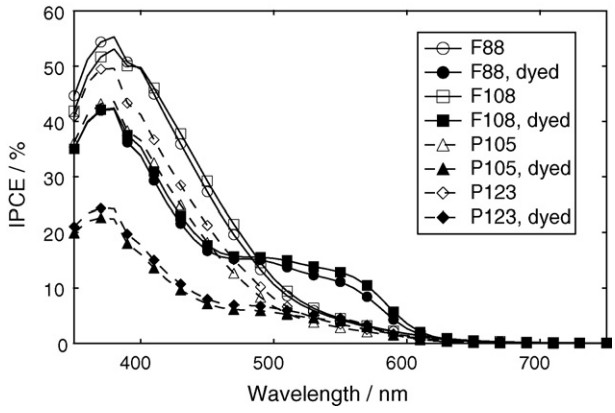

Fig. 9. Photocurrent action spectra of solar cells with the I_3^- rich electrolyte and the dyed or non-dyed NiO electrodes prepared using different polymer templates.

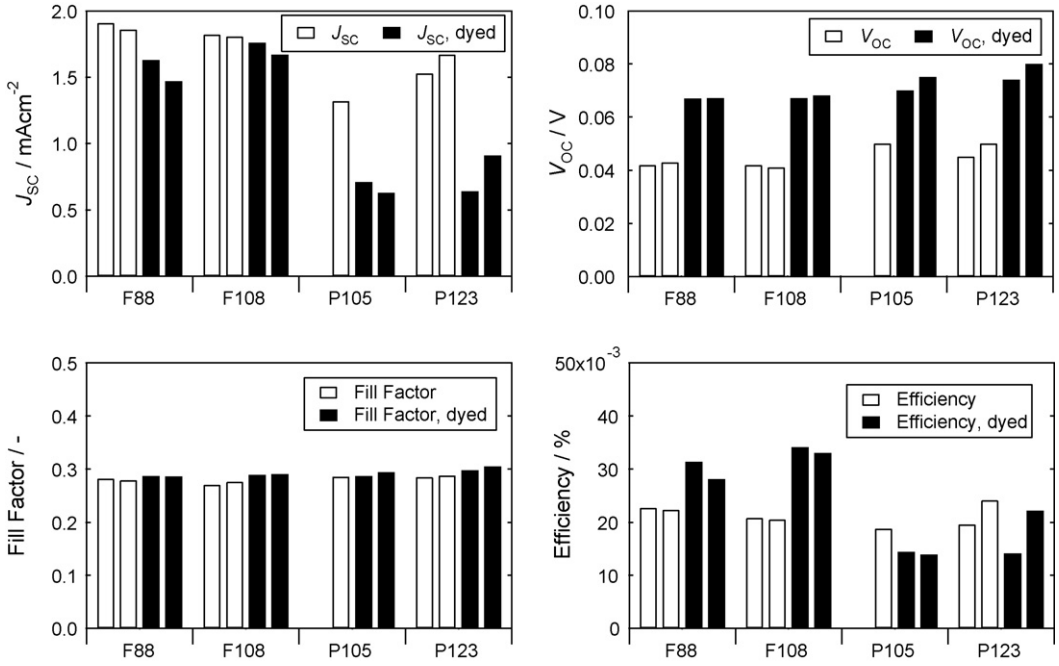

Fig. 10. *I–V* performances of the solar cells with the I_3^- rich electrolyte and the dyed and non-dyed NiO electrodes prepared using different polymer templates. One of the two non-dyed F105 cells did not function as a photovoltaic cell due to some failure during cell preparation.

trolyte instead of I^- rich one. We tentatively explain this result as follows. At 500 nm, NiO absorbs appreciable amount of light as shown in Fig. 3, indicating the existence of sites at intra-band-gap levels. With the low concentration of I_3^- in the I^- rich electrolyte, however, the photo-excited electrons hardly transferred to I_3^-. On the other hand, the high concentration of I_3^- in the I_3^- rich electrolyte enhanced the electron transfer from the intra-band-gap level to I_3^-, resulting in 12% IPCE.

Dye-sensitization IPCE cannot be separated from direct excitation IPCE at around 500 nm. Seemingly, dye-sensitization and direct excitation is not additive, and then applying the I_3^- rich electrolyte did not increase IPCE at around 500 nm.

V_{OC} decreased by around 15 mV when the I_3^- rich electrolyte was used instead of the I^- rich one, probably because the redox potential of the I_3^- rich electrolyte is more positive than that of the I^- rich one, which reduces the potential difference between the NiO valence band edge and the redox potential of the electrolyte. This decrease in V_{OC} cancelled the effect of the current increase due to the enhanced direct excitation IPCE, and as a result, the cell efficiency was not improved by using I_3^- rich electrolyte.

4. Conclusion

In order to prepare better NiO film electrode for dye-sensitization, a polymer templating method was applied. The dye NK-2684 was used as a standard dye for evaluating NiO films as electrode for dye-sensitized solar cells. Among the nonionic triblock co-polymers (PEO–PPO–PEO) examined as templates for preparing nanoporous NiO film electrode of p-type dye-sensitized solar cells, those with high PEO/PPO ratio leaded to two-fold higher dye-sensitization IPCE in comparison with low PEO/PPO polymers. Use of high PEO/PPO templates resulted in NiO membrane structure formed by uniformly distributed nano particles and pores with small pore volume, giving large surface area for dye adsorption, while low PEO/PPO templates resulted in large pore volume.

References

[1] B. O'Regan, M. Grätzel, Nature 353 (1991) 737–740.
[2] M.K. Nazeeruddin, F. De Angelis, S. Fantacci, A. Selloni, G. Viscardi, P. Liska, S. Ito, T. Bessho, M. Grätzel, J. Am. Chem. Soc. 127 (2005) 16835–16847.
[3] M. Dürr, A. Bamedi, A. Yasuda, G. Nelles, Appl. Phys. Lett. 84 (2004) 3397–3399.
[4] W. Kubo, A. Sakamoto, T. Kitamura, Y. Wada, S. Yanagida, J. Photochem, Photobiol. A: Chem. 164 (2004) 33–39.
[5] J. He, H. Lindström, A. Hagfeldt, S.-E. Lindquist, Sol. Energy Mater. Sol. Cells 62 (2000) 265–273.
[6] J. He, H. Lindström, A. Hagfeldt, S.-E. Lindquist, J. Phys. Chem. B 103 (1999) 8940–8943.
[7] A. Nakasa, H. Usami, S. Sumikura, S. Hasegawa, T. Koyama, E. Suzuki, Chem. Lett. 34 (2005) 500–501.
[8] Y. Saito, S. Kambe, T. Kitamura, Y. Wada, S. Yanagida, Sol. Energy Mater. Sol. Cells 83 (2004) 1–13.
[9] D. Zhao, Q. Huo, J. Feng, B.F. Chmelka, G.D. Stucky, J. Am. Chem. Soc. 120 (1998) 6024–6036.
[10] L. Zhang, J.C. Yu, Chem. Commun. (2003) 2078–2079.
[11] Y. Shimizu, A. Jono, T. Hyodo, M. Egashira, Sens. Actuators B 108 (2005) 56–61.
[12] G. Boschloo, A. Hagfeldt, J. Phys. Chem. B 105 (2001) 3039–3044.
[13] A. Hagfeldt, M. Grätzel, Chem. Rev. 95 (1995) 49–68.
[14] T. Sakata, K. Hashimoto, M. Hiramoto, J. Phys. Chem. 94 (1990) 3040–3045.